DOI: 10.11844/cjcb.2025.05.0004
中国细胞生物学学报 Chinese Journal of Cell Biology 2025, 47(5): 1017–1025 CSTR: 32200.14.cjcb.2025.05.0004

MiR-17-5p调控PPARγ/ABCA1信号通路对ox-LDL诱导的血管内皮细胞损伤的影响

徐航[1] 张富龙[2] 王欢[3]*

([1]空军军医大学西京医院心血管内科, 西安 710032; [2]西安国际医学中心医院心血管内科, 西安 710061;
[3]空军军医大学西京医院急诊科, 西安 710032)

摘要 该文旨在探究miR-17-5p调控过氧化物酶体增殖激活受体-γ(PPARγ)/ATP结合盒转运蛋白A1(ABCA1)信号通路对氧化低密度脂蛋白(ox-LDL)诱导的血管内皮细胞损伤的影响。将人主动脉内皮细胞(HAEC)分为对照(control)组、ox-LDL组、inhibitor NC组、miR-17-5p inhibitor组、miR-17-5p inhibitor+GW9662组, 除control组外其他组均利用ox-LDL诱导HAEC损伤。CCK-8法检测HAEC增殖情况; 流式细胞术检测HAEC凋亡情况; 血管形成实验检测血管形成情况; 试剂盒测定HAEC中丙二醛(MDA)、超氧化物歧化酶(SOD)、谷胱甘肽过氧化物酶(GSH-Px)活性; qRT-PCR检测HAEC中miR-17-5p、*PPARγ*和*ABCA1* mRNA表达水平; Western blot分析HAEC中PPARγ和ABCA1蛋白表达水平; 双荧光素酶报告基因检测miR-17-5p与*ABCA1*的相互关系。与control组相比, ox-LDL组HAEC的D_{450}值降低, SOD和GSH-Px活性降低, PPARγ、ABCA1 mRNA及蛋白表达水平均降低, 凋亡率以及miR-17-5p和MDA水平升高, 血管形成数量减少(P<0.05); 与inhibitor NC组相比, miR-17-5p inhibitor组HAEC的D_{450}值升高, SOD和GSH-Px活性提高, PPARγ、ABCA1 mRNA及蛋白表达水平均提高, 凋亡率以及miR-17-5p和MDA水平降低, 血管形成数量增加(P<0.05); 与miR-17-5p inhibitor组相比, miR-17-5p inhibitor+GW9662组HAEC的D_{450}值降低, SOD和GSH-Px活性降低, PPARγ、ABCA1 mRNA及蛋白表达水平均降低, 凋亡率和MDA水平升高, 血管形成数量减少(P<0.05)。miR-17-5p可能通过抑制PPARγ/ABCA1信号通路加剧ox-LDL诱导的HAEC损伤。

关键词 miR-17-5p; 过氧化物酶体增殖激活受体-γ/ATP结合盒转运蛋白A1; 氧化低密度脂蛋白; 血管内皮细胞; 人主动脉内皮细胞

The Effect of MiR-17-5p on ox-LDL-Induced Endothelial Cell Injury by Regulating the PPARγ/ABCA1 Signaling Pathway

XU Hang[1], ZHANG Fulong[2], WANG Huan[3]*

([1]*Department of Cardiovascular Medicine, Xijing Hospital of Air Force Medical University, Xi'an 710032, China*;
[2]*Department of Cardiovascular Medicine, Xi'an International Medical Center Hospital, Xi'an 710061, China*;
[3]*Department of Emergency, Xijing Hospital of Air Force Medical University, Xi'an 710032, China*)

Abstract This study aims to investigate the effect of miR-17-5p on ox-LDL (oxidized low-density lipoprotein)-induced vascular endothelial cell injury by regulating the PPARγ (peroxisome proliferator activated receptor-γ)/ABCA1 (ATP binding cassette transporter A1) signaling pathway. HAEC (human aortic endothelial cell) were assigned into control group, ox-LDL group, inhibitor NC group, miR-17-5p inhibitor group, and miR-17-5p inhibitor+GW9662 group. All other groups except the control group were induced HAEC injury using ox-

收稿日期: 2024-12-17 接受日期: 2025-01-17
*通信作者。Tel: 18192703560, E-mail: 987365769@qq.com
Received: December 17, 2024 Accepted: January 17, 2025
*Corresponding author. Tel: +86-18192703560, E-mail: 987365769@qq.com

LDL. CCK-8 method was used to detect HAEC proliferation. Flow cytometry was used to detect HAEC apoptosis. The angiogenesis experiment detected the angiogenesis. Reagent kits were used to determine the activities of MDA (malondialdehyde), SOD (superoxide dismutase), and GSH-Px (glutathione peroxidase) in HAEC. qRT-PCR was used to detect the mRNA expression levels of miR-17-5p, *PPARγ*, and *ABCA1* in HAEC. Western blot was used to analyze PPARγ and ABCA1 protein levels in HAEC. Dual luciferase reporter gene was used to detect the relationship between miR-17-5p and *ABCA1*. Compared with the control group, the D_{450} value of HAEC in the ox-LDL group was reduced, the SOD and GSH-Px activities decreased, the expression levels of PPARγ, ABCA1 mRNAs and proteins decreased, while the apoptosis rate, miR-17-5p, and MDA levels increased, blood vessel formation reduced (P<0.05). Compared with the inhibitor NC group, the D_{450} value of HAEC in miR-17-5p inhibitor group was increased, the SOD and GSH-Px activities increased, PPARγ, ABCA1 mRNA and protein expression increased, while the apoptosis rate, miR-17-5p and MDA levels reduced, blood vessel formation increased (P<0.05). Compared with the miR-17-5p inhibitor group, the D_{450} value of HAEC in miR-17-5p inhibitor+GW9662 group was reduced, the SOD and GSH-Px activities decreased, the expression levels of PPARγ, ABCA1 mRNAs and proteins decreased, while the apoptosis rate, miR-17-5p, and MDA levels increased, blood vessel formation reduced (P<0.05). MiR-17-5p may exacerbate ox-LDL-induced HAEC injury by inhibiting the PPARγ/ABCA1 signaling pathway.

Keywords miR-17-5p; peroxisome proliferator activated receptor-γ/ATP binding cassette transporter A1; oxidized low-density lipoprotein; vascular endothelial cells; human aortic endothelial cell

动脉粥样硬化是一种大中型动脉内的慢性炎症和脂质沉积性疾病，可导致冠状动脉疾病、心肌梗死、中风和外周动脉疾病等心血管疾病，在初始阶段，血管内皮功能障碍能够触发斑块的形成和动脉粥样硬化病变的形成[1-2]。内皮在维持生理结构和功能方面发挥着重要作用。内皮细胞形成单层，产生调节血管张力、炎症、血液凝固、血管细胞生长和死亡、血管生成、白细胞迁移和防止血小板黏附的因子[3]。因此，探索血管内皮细胞损伤的分子机制对于治疗动脉粥样硬化非常有价值。过氧化物酶体增殖激活受体-γ(peroxisome proliferator activated receptor-γ, PPARγ)促进脂肪酸的吸收、甘油三酯的形成和在脂滴中的储存，从而增加胰岛素敏感性和促进葡萄糖代谢，其可对血管壁和免疫细胞发挥抗动脉粥样硬化和抗炎作用[4]。研究显示，刺芒柄花素通过刺激PPARγ信号转导保护人脐静脉内皮细胞免受氧化低密度脂蛋白(oxidized low-density lipoprotein, ox-LDL)诱导的内皮功能障碍[5]。组蛋白脱乙酰酶3通过调控miR-19b/PPARγ/核因子κB(nuclear factor kappa-B, NF-κB)轴来预防动脉粥样硬化[6]。ATP结合盒转运蛋白A1(ATP binding cassette transporter A1, ABCA1)除了通过与载脂蛋白A-I结合介导胆固醇外排外，还能增加膜联蛋白A1(annexin A1, ANXA1)的表达水平并将其从细胞质转运到细胞膜。ANXA1还可以通过充当磷脂酶A_2抑制蛋白或增加PPARγ和IL-10的表达水平来增加ABCA1表达水平和促进胆固醇外排。ABCA1、PPARγ和ANXA1可能形成反馈回路并相互调节[7]。芪参益气丸通过激活胆固醇反向转运通路PPARγ-肝脏X受体α/β(liver X receptors α/β, LXRα/β)-ABCA1通路抑制动脉粥样硬化[8]。长链非编码RNA MALAT1通过miR-17-5p/ABCA1轴调节ox-LDL诱导的巨噬细胞中的胆固醇积累[9]。在此背景下，Starbase分析显示miR-17-5p与*ABCA1*有互补结合序列，因此，本研究通过ox-LDL诱导人主动脉内皮细胞(human aortic endothelial cell, HAEC)损伤，分析miR-17-5p靶向PPARγ/ABCA1信号通路对HAEC损伤的影响。

1 材料与方法

1.1 细胞来源

HAEC(货号：JNO-H0514)购自广州吉妮欧生物科技有限公司。

1.2 主要试剂

Inhibitor NC、miR-17-5p inhibitor质粒购自广州市锐博生物科技有限公司；GW9662(货号：HY-16578)购自MedChem Express公司；人源ox-LDL(货号：MP6010-2MG)购自上海懋康生物科技有限公司；丙二醛(malondialdehyde, MDA)含量检测试剂盒(货

号: BC0020)、超氧化物歧化酶(superoxide dismutase, SOD)活性检测试剂盒(货号: BC0170)、谷胱甘肽过氧化物酶(glutathione peroxidase, GSH-Px/GPX)活性检测试剂盒(货号: BC1190)购自北京索莱宝科技有限公司; Trizol(总RNA抽提试剂, 货号: R0016)、超敏ECL化学发光试剂盒(货号: P0018S)、双荧光素酶报告基因检测试剂盒(货号: 11402ES80)、Hoechst染色试剂盒(货号: C0003)购自上海碧云天生物技术有限公司; microRNA逆转录试剂盒(货号: MR101-01)、cDNA一链合成试剂盒(货号: R412-01)、探针法定量PCR检测试剂盒(货号: Q112-02)购自南京诺唯赞生物科技股份有限公司; Annexin V-FITC/PI细胞凋亡检测试剂盒(货号: E-CK-A211)购自武汉伊莱瑞特生物科技股份有限公司; 超敏型细胞增殖检测试剂(货号: BMU106-CN)购自亚科因生物技术有限公司; RIPA裂解缓冲液(货号: MT0066)购自北京百奥莱博科技有限公司; Lipofectamine™ 3000转染试剂(货号: L3000001)购自ThermoFisher Scientific公司; GAPDH兔单克隆抗体(货号: ab128915)、PPARγ兔单克隆抗体(货号: ab272718)、ABCA1兔单克隆抗体(货号: ab307534)和山羊抗兔IgG二抗(HRP标记, 货号: ab205718)购自Abcam公司。

1.3 方法

1.3.1 细胞转染分组与ox-LDL模型构建 将HAEC细胞分为对照(control)组、ox-LDL组、inhibitor NC组、miR-17-5p inhibitor组、miR-17-5p inhibitor+GW9662组, control组和ox-LDL组不转染质粒, inhibitor NC组转染inhibitor NC质粒, miR-17-5p inhibitor组和miR-17-5p inhibitor+GW9662组转染miR-17-5p inhibitor质粒, miR-17-5p inhibitor+GW9662组转染后立即用5 μmol/L PPARγ拮抗剂GW9662培养[5]。用Lipofectamine™ 3000转染试剂进行质粒转染, 转染24 h后用100 mg/L ox-LDL培养HAEC细胞24 h[10], 模拟体外动脉粥样硬化。

1.3.2 CCK-8法检测HAEC细胞增殖情况 将HAEC接种到96孔板(100 μL/孔)中, 转染48 h后, 在每孔中加入10 μL CCK-8溶液, 注意不要产生气泡。然后将细胞在37 °C、5% CO_2培养箱中孵育4 h, 通过酶标仪测量450 nm波长处的吸光度(*D*)值。

1.3.3 Hoechst染色观察HAEC细胞凋亡情况 96孔板培养细胞48 h后, 去除培养液, 加入50 μL固定液, 室温固定10 min, 去除固定液, 用PBS洗2次, 加入50 μL Hoechst 33258染色液室温染色5 min。去除染色液, 用PBS洗2次, 每次3 min, 吸尽液体, 抗荧光淬灭封片液封片, 荧光显微镜下观察细胞凋亡情况。

1.3.4 流式细胞术检测HAEC细胞凋亡情况 收获的HAEC细胞用PBS洗涤1次, 在4 ℃下以1 000 ×*g*离心5 min后弃上清, 加入100 μL 1× Annexin V结合缓冲液重悬细胞, 细胞悬液中加入2.5 μL的Annexin V-FITC试剂和2.5 μL的PI试剂(50 μg/mL), 涡旋混匀后, 室温避光孵育15~20 min。加入400 μL 1× Annexin V结合缓冲液, 混匀。然后使用FACSCanto FCM流式细胞仪对HAEC细胞进行流式细胞术分析, 使用FlowJo软件进行数据分析。

1.3.5 血管形成实验 预先用基质胶包被96孔板, 并在37 °C下放置1 h使其凝固。然后将饥饿处理的HAEC接种到每个孔中, 加入1% FBS并于37 °C下孵育6 h。最后, 观察、成像并分析HAEC的血管形成情况。

1.3.6 HAEC细胞中的MDA含量、SOD和GSH-Px活性测定 超声破碎(功率200 W, 超声3 s, 间隔10 s, 重复30次)裂解HAEC, 细胞裂解液在4 ℃下以8 000 ×*g*离心10 min。然后, 收集上清液并置于冰上进行后续检测。对于MDA含量, 将所得上清液与MDA检测工作液混合, 在100 ℃下保持60 min, 冷却至室温, 在10 000 ×*g*下离心10 min, 于532和600 nm波长处测定每个样品的吸光度(*D*)值, 计算MDA含量, 以control组为标准得出MDA相对含量, SOD和GSH-Px相对活性计算方式相同。对于SOD活性, 将所得上清液与SOD工作液充分混合, 37 ℃下放置30 min, 然后测量560 nm波长处的吸光度值, 根据公式: 抑制率=[(Δ*D*空白–Δ*D*样品)/Δ*D*空白]×100%, 计算SOD的抑制率及相对SOD活性。对于GSH-Px活性, 将所得上清液与GSH-Px工作液充分混合, 室温下放置15 min, 然后测量412 nm波长处的吸光度值, 根据公式: 抑制率=[(*D*对照–*D*样品)/(*D*对照–*D*空白)]×100%, 计算GSH-Px的抑制率及相对GSH-Px活性。

1.3.7 qRT-qPCR检测miR-17-5p、*PPARγ*和*ABCA1*表达水平 利用Trizol提取HAEC细胞的总RNA。使用NanoDrop 2000 UV-Vis分光光度计分析总RNA浓度, 并使用miRNA逆转录专用试剂盒和cDNA一链合成试剂盒将RNA转录为cDNA。使用cDNA和AceQ qPCR Probe Master Mix进行实时PCR检测, 使用以下条件进行循环: 95 °C预变性2 min; 95 °C变性30 s, 60 °C退火1 min, 68 °C延伸30 s, 40个循环。以*β-actin*和*U6*作为内参, 采用$2^{-\Delta\Delta Ct}$法对数据

进行分析。qRT-PCR所用的引物由武汉金开瑞生物工程有限公司合成，引物序列如下：*U6*上游引物5′-GCT TCG GCA GCA CAT ATA CT-3′，下游引物5′-GCA GGG TCC GAG GTA TTC-3′；*PPARγ*上游引物5′-GCA GTG GGG ATG TCT CAT AAT GC-3′，下游引物5′-CAG GGG GGT GAT GTG TTT GAA-3′；*ABCA1*上游引物5′-CCC TGT GGA ATG TAC CTA TGT G-3′，下游引物5′-GAG GTG TCC CAA AGA TGC AA-3′；*GAPDH*上游引物5′-GAC CTG ACC TGC CGT CTA G-3′，下游引物5′-AGG AGT GGG TGT CGC TGT-3′；miR-17-5p上游引物5′-CAA AGT GCT TAC AGT GCA GGT AG-3′，下游引物5′-GCA GGG TCC GAG GTA TTC-3′。

1.3.8 Western blot检测PPARγ和ABCA1蛋白表达情况 用含有蛋白酶和磷酸酶抑制剂的RIPA裂解缓冲液提取不同组别的HAEC总蛋白。在4 ℃下以12 000 ×*g*离心5 min后，用10% SDS-PAGE电泳分离蛋白质并将其转移到聚偏氟乙烯膜上。然后在4 ℃下用50 g/L脱脂牛奶封闭膜12 h，并与GAPDH(1:10 000)、PPARγ(1:1 000)和ABCA1(1:1 000)一抗在4 ℃下孵育过夜。然后将膜与二抗(1:50 000，HRP标记的山羊抗兔IgG抗体)在37 ℃下孵育2 h。使用超敏ECL化学发光试剂盒进行显色。最后以β-actin为内参，使用Quantity One扫描软件分析相对灰度值，计算PPARγ和ABCA1相对表达水平。

1.3.9 双荧光素酶报告基因检测miR-17-5p与*ABCA1*的靶向关系 使用Starbase(https://rnasysu.com/encori/agoClipRNA.php?source=mRNA&flag)确定miR-17-5p与*ABCA1*的靶向位点。将含有结合位点的ABCA1序列插入pmirGLO载体获得ABCA1野生型(WT)质粒，定点诱变ABCA1野生序列并生成ABCA1突变型(MUT)质粒，将ABCA1-WT/MUT质粒分别与miR-NC、miR-17-5p mimic质粒共转染HAEC细胞，48 h后，通过双荧光素酶活性判断miR-17-5p与*ABCA1*的靶向关系。

1.4 统计学分析

实验数据用平均数±标准差($\bar{x}\pm s$)表示，利用GraphPad Prism 7.0软件进行统计分析，两组比较采用*t*检验，多组间比较采用单因素方差分析，进一步组间比较采用SNK-*q*检验。$P<0.05$表示差异有统计学意义。

2 结果

2.1 各组HAEC增殖比较

与control组相比，ox-LDL组HAEC细胞D_{450}值降低($P<0.05$)；与inhibitor NC组比较，miR-17-5p inhibitor组HAEC细胞D_{450}值升高($P<0.05$)；与miR-17-5p inhibitor组比较，miR-17-5p inhibitor+GW9662组HAEC细胞D_{450}值降低($P<0.05$)，见表1。

2.2 各组HAEC细胞Hoechst染色

与control组相比，ox-LDL组可见较多细胞凋亡，细胞核碎裂，呈现亮蓝色；与inhibitor NC组比较，miR-17-5p inhibitor组细胞凋亡减少；与miR-17-5p inhibitor组比较，miR-17-5p inhibitor+GW9662组细胞凋亡增加，见图1。

2.3 各组HAEC细胞凋亡率比较

与control组相比，ox-LDL组HAEC细胞凋亡率提高($P<0.05$)；与inhibitor NC组比较，miR-17-5p inhibitor组HAEC细胞凋亡率降低($P<0.05$)；与miR-17-5p inhibitor组比较，miR-17-5p inhibitor+GW9662组HAEC细胞凋亡率升高($P<0.05$)，见图2与表2。

2.4 各组HAEC细胞血管形成实验

与control组相比，ox-LDL组HAEC血管形成数量减少($P<0.05$)；与inhibitor NC组比较，miR-17-5p inhibitor组HAEC血管形成数量增加

表1 各组HAEC的D_{450}值比较

Table 1 Comparison of D_{450} values of HAEC in each group

分组 Groups	D_{450}值 D_{450} value
Control	1.86±0.21
ox-LDL	1.21±0.14*
Inhibitor NC	1.23±0.15
miR-17-5p inhibitor	1.64±0.18$^{\#}$
miR-17-5p inhibitor+GW9662	1.35±0.15$^{\&}$

*$P<0.05$，与control组相比；$^{\#}P<0.05$，与inhibitor NC组相比；$^{\&}P<0.05$，与miR-17-5p inhibitor组相比。

*$P<0.05$ compared with control group; $^{\#}P<0.05$ compared with inhibitor NC group; $^{\&}P<0.05$ compared with miR-17-5p inhibitor group.

(P<0.05); 与miR-17-5p inhibitor组比较, miR-17-5p inhibitor+GW9662组HAEC血管形成数量减少(P<0.05), 见图3与表3。

2.5 各组HAEC中MDA含量及SOD、GSH-Px活性

与control组相比, ox-LDL组HAEC中MDA含量

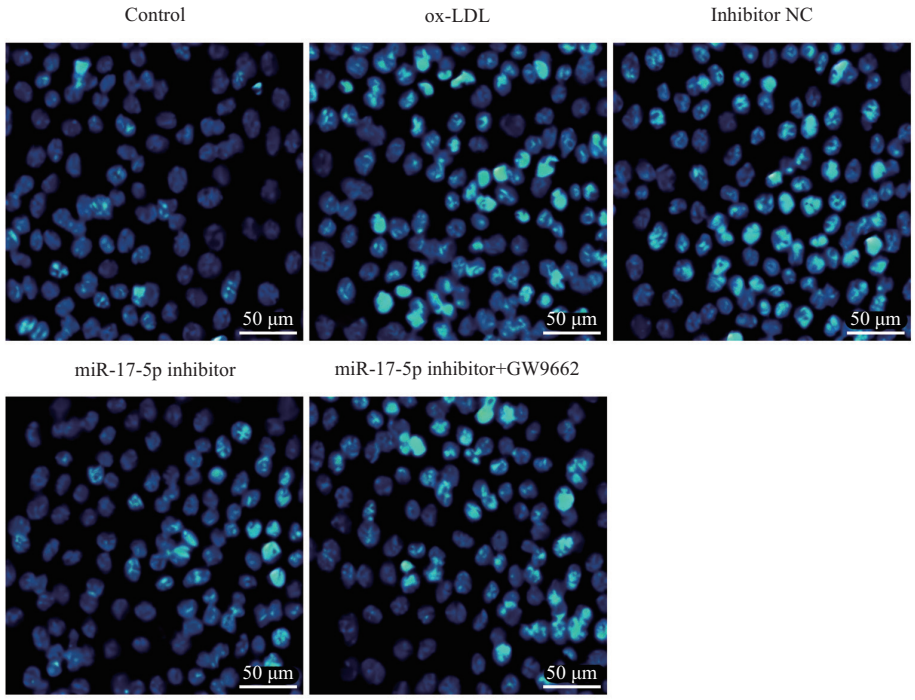

图1 各组HAEC细胞Hoechst染色情况

Fig.1 Hoechst staining of HAEC cells in each group

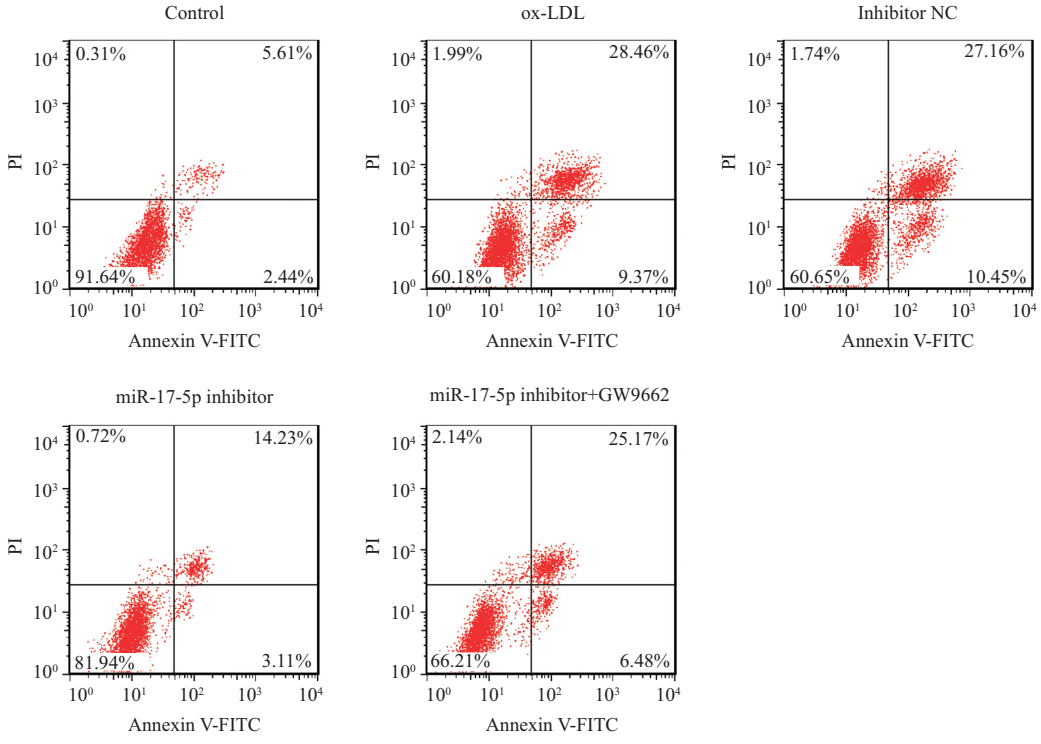

图2 各组HAEC凋亡的流式分析图

Fig.2 Flow cytometry analysis of HAEC apoptosis in each group

升高, SOD和GSH-Px活性降低(P<0.05); 与inhibitor NC组比较, miR-17-5p inhibitor组HAEC中MDA含量降低, SOD和GSH-Px活性升高(P<0.05); 与miR-17-5p inhibitor组比较, miR-17-5p inhibitor+GW9662组HAEC中MDA含量升高, SOD和GSH-Px活性降低(P<0.05), 见表4。

2.6 各组HAEC中miR-17-5p、*PPARγ*和*ABCA1* mRNA表达水平

与control组相比, ox-LDL组HAEC中miR-17-

表2 各组HAEC凋亡率比较

Table 2 Comparison of HAEC apoptosis rate in each group

分组 Groups	细胞凋亡率/% Cell apoptosis rate /%
Control	8.48±0.96
ox-LDL	36.23±3.89*
Inhibitor NC	37.26±3.95
miR-17-5p inhibitor	17.47±1.94$^{\#}$
miR-17-5p inhibitor+GW9662	30.48±3.26$^{\&}$

*P<0.05, 与control组相比; $^{\#}P$<0.05, 与inhibitor NC组相比; $^{\&}P$<0.05, 与miR-17-5p inhibitor组相比。

*P<0.05 compared with control group; $^{\#}P$<0.05 compared with inhibitor NC group; $^{\&}P$<0.05 compared with miR-17-5p inhibitor group.

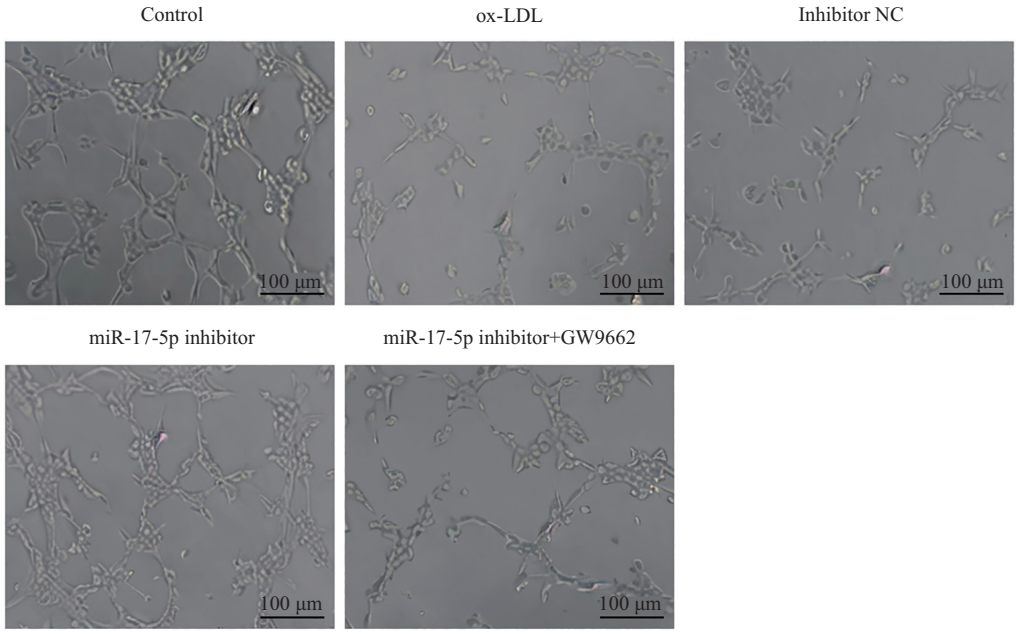

图3 各组HAEC血管形成照片

Fig.3 Photographs of HAEC blood vessel formation in each group

表3 各组HAEC细胞血管形成数量比较

Table 3 Comparison of the number of blood vessel formation in HAEC cells in each group

分组 Groups	血管形成数量 The number of blood vessel formation
Control	9.86±1.32
ox-LDL	4.52±0.78*
Inhibitor NC	4.48±0.61
miR-17-5p inhibitor	8.13±1.02$^{\#}$
miR-17-5p inhibitor+GW9662	5.25±0.69$^{\&}$

*P<0.05, 与control组相比; $^{\#}P$<0.05, 与inhibitor NC组相比; $^{\&}P$<0.05, 与miR-17-5p inhibitor组相比。

*P<0.05 compared with control group; $^{\#}P$<0.05 compared with inhibitor NC group; $^{\&}P$<0.05 compared with miR-17-5p inhibitor group.

表4 HAEC中MDA含量及SOD、GSH-Px活性

Table 4 MDA content and SOD, GSH-Px activities in HAEC

分组 Groups	MDA	SOD	GSH-Px
Control	1.02±0.11	1.05±0.11	1.03±0.11
ox-LDL	6.36±0.67*	0.18±0.03*	0.14±0.02*
Inhibitor NC	6.42±0.68	0.19±0.03	0.15±0.03
miR-17-5p inhibitor	2.41±0.25$^{\#}$	0.59±0.07$^{\#}$	0.53±0.06$^{\#}$
miR-17-5p inhibitor+GW9662	5.57±0.59$^{\&}$	0.32±0.04$^{\&}$	0.28±0.03$^{\&}$

*P<0.05, 与control组相比; $^{\#}P$<0.05, 与inhibitor NC组相比; $^{\&}P$<0.05, 与miR-17-5p inhibitor组相比。

*P<0.05 compared with control group; $^{\#}P$<0.05 compared with inhibitor NC group; $^{\&}P$<0.05 compared with miR-17-5p inhibitor group.

表5 HAEC中miR-17-5p、*PPARγ*和*ABCA1* mRNA表达比较

Table 5 Comparison of miR-17-5p, *PPARγ*, *ABCA1* mRNA expression in HAEC

分组 Groups	miR-17-5p	*PPARγ*	*ABCA1*
Control	1.06±0.11	1.04±0.11	1.07±0.11
ox-LDL	3.64±0.37*	0.33±0.04*	0.29±0.03*
Inhibitor NC	3.55±0.38	0.32±0.04	0.30±0.04
miR-17-5p inhibitor	1.66±0.19$^{\#}$	0.67±0.07$^{\#}$	0.69±0.08$^{\#}$
miR-17-5p inhibitor+GW9662	1.63±0.17	0.48±0.06$^{\&}$	0.46±0.05$^{\&}$

*P<0.05, 与control组相比; $^{\#}P$<0.05, 与inhibitor NC组相比; $^{\&}P$<0.05, 与miR-17-5p inhibitor组相比。

*P<0.05 compared with control group; $^{\#}P$<0.05 compared with inhibitor NC group; $^{\&}P$<0.05 compared with miR-17-5p inhibitor group.

5p水平升高, *PPARγ*和*ABCA1* mRNA表达水平降低(P<0.05); 与inhibitor NC组比较, miR-17-5p inhibitor组HAEC中miR-17-5p水平降低, *PPARγ*和*ABCA1* mRNA表达水平增加(P<0.05); 与miR-17-5p inhibitor组比较, miR-17-5p inhibitor+GW9662组HAEC中*PPARγ*和*ABCA1* mRNA表达水平降低(P<0.05), 见表5。

2.7 各组HAEC中PPARγ、ABCA1蛋白表达水平

与control组相比, ox-LDL组HAEC中PPARγ、ABCA1蛋白表达水平降低(P<0.05); 与inhibitor NC组比较, miR-17-5p inhibitor组HAEC中PPARγ、ABCA1蛋白表达水平升高(P<0.05); 与miR-17-5p inhibitor组比较, miR-17-5p inhibitor+GW9662组HAEC中PPARγ、ABCA1蛋白表达水平降低(P<0.05), 见图4。

2.8 miR-17-5p与*ABCA1*的相互关系

Starbase分析显示miR-17-5p与*ABCA1*具有互补结合序列, 见图3。双荧光素酶活性检测结果表明, 与ABCA1-WT和miR-NC共转染比较, ABCA1-WT和miR-17-5p mimic共转染HAEC后, 荧光素酶的活性明显降低(P<0.05), 见图5和表6。

3 讨论

动脉粥样硬化是由动脉内胆固醇含量丰富的斑块慢性积累造成的。动脉粥样硬化性心血管疾病是高收入国家的主要死亡原因, 血管内皮位于体循环和下层血管壁的界面, 在动脉粥样硬化形成的病理生理过程调控中起着重要作用[11]。动脉粥样硬化的发展主要归因于血管壁中脂质和炎性碎片的积累, 也与巨噬细胞、平滑肌细胞和内皮细胞的凋亡有关[12]。血管内皮是血管的内层, 在维持血管完整性和体内平衡方面起着核心作用, 并与血流直接接触, 血管内皮细胞在血流稳态维持中发挥着关键作用[13]。在血流诱导性动脉粥样硬化小鼠模型中, 血流紊乱会原位重编程动脉内皮细胞, 使其从健康表型转变为患病细胞, 特征是表现出内皮炎症、内皮细胞向间质细胞转化、内皮细胞向免疫细胞样转化和代谢变化[14]。

已有研究表明, miR-17-5p是冠状动脉粥样硬化的生物标志物, miR-17也是与动脉粥样硬化相关的5种miRNA之一[15]。研究表明, p53依赖性的lincRNA-p21通过下调miR-17-5p, 从而上调SIRT7来防止动脉粥样硬化中血管平滑肌细胞的增殖并促进凋亡[16]。circDENND1B通过调控miR-17-5p/ABCA1轴促进胆

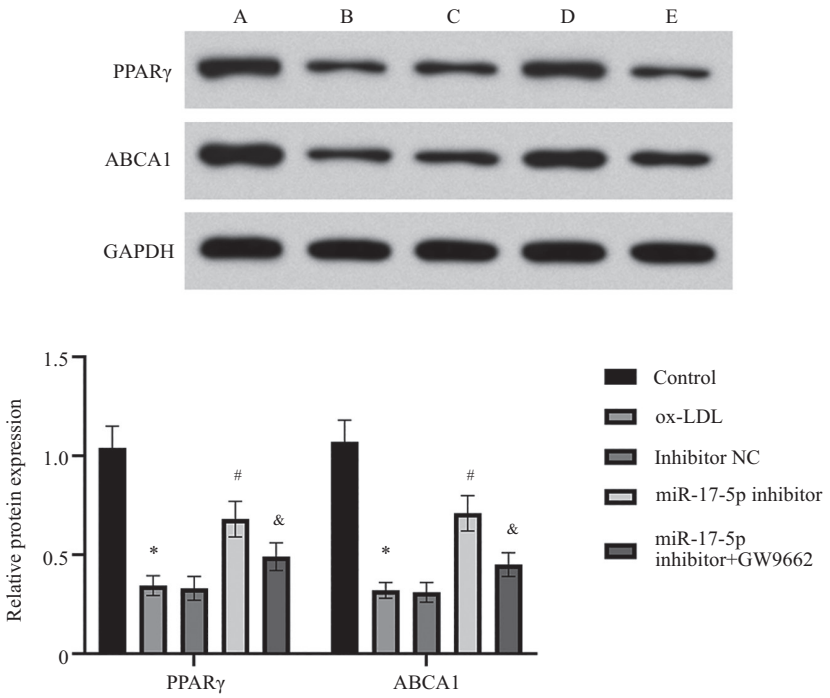

A: control组; B: ox-LDL组; C: inhibitor NC组; D: miR-17-5p inhibitor组; E: miR-17-5p inhibitor+GW9662组。*P<0.05, 与control组相比; #P<0.05, 与inhibitor NC组相比; &P<0.05, 与miR-17-5p inhibitor组相比。

A: control group; B: ox-LDL group; C: inhibitor NC group; D: miR-17-5p inhibitor group; E: miR-17-5p inhibitor+GW9662 group. *P<0.05 compared with control group; #P<0.05 compared with inhibitor NC group; &P<0.05 compared with miR-17-5p inhibitor group.

图4 各组HAEC中PPARγ、ABCA1蛋白条带及表达比较

Fig.4 Comparison of PPARγ and ABCA1 protein bands and expression in HAEC of each group

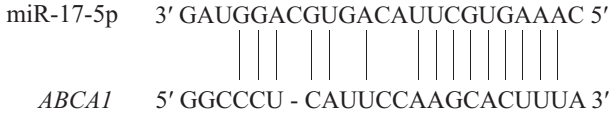

图5 miR-17-5p与*ABCA1*靶向结合位点预测

Fig.5 Prediction of target binding sites of miR-17-5p and *ABCA1*

表6 双荧光素酶活性检测结果

Table 6 Results of dual luciferase activity detection

分组 Groups	ABCA1-WT	ABCA1-MUT
miR-NC	1.06±0.11	1.07±0.12
miR-17-5p mimic	0.54±0.06	1.03±0.11
t	10.116	0.602
P	0.000	0.561

固醇外流, 参与IL-1β单克隆抗体在小鼠体内的抗动脉粥样硬化作用[17]。LncRNA NEAT1通过调控miR-17-5p/Itchy E3泛素蛋白连接酶/肝激酶B1轴促进泡沫细胞形成和动脉粥样硬化进展[18]。本研究发现, ox-LDL诱导导致HAEC的增殖能力降低, 凋亡率和miR-17-5p水平升高, 氧化应激加重, 与前人研究结果[15-16]一致; 在抑制HAEC的miR-17-5p表达后, 细胞增殖能力提高, 凋亡率降低, 氧化应激被抑制; 提示, 抑制miR-17-5p水平可减轻ox-LDL诱导的HAEC损伤。

PPARγ是核受体超家族的成员, 是研究最广泛的配体诱导转录因子之一。自20世纪90年代初被发现以来, PPARγ已被证明在脂肪细胞分化中具有关键作用[19]。研究发现, 松果菊苷激活Nrf2/PPARγ信号通路, 调节线粒体融合–裂变平衡, 改善ox-LDL诱

导的冠状动脉内皮细胞功能障碍[20]。三七皂苷Fc在体外减轻ox-LDL诱导的内皮细胞功能障碍并上调PPARγ表达[21]。MiR-33-5p通过调节柠檬酸盐合酶和ABCA1抑制血管内皮细胞中的胆固醇外流[22]。Starbase分析发现, miR-17-5p与*ABCA1*存在互补结合区域。本研究中, 抑制miR-17-5p表达可引起*ABCA1*表达水平升高, 而抑制miR-17-5p的同时加入PPARγ拮抗剂发现, HAEC中*PPARγ*、*ABCA1*表达水平及细胞增殖能力均降低, 凋亡率升高, 氧化应激加重; 且双荧光素酶实验验证显示, miR-17-5p与*ABCA1*具有靶向关系, 提示抑制miR-17-5p水平可能通过促进*PPARγ*和*ABCA1*表达, 减轻ox-LDL诱导的HAEC损伤。

综上, miR-17-5p可能通过抑制PPARγ/ABCA1信号通路促进ox-LDL诱导的HAEC细胞损伤。本实验提示miR-17-5p可能成为动脉粥样硬化的治疗靶点之一, 但未进行动物实验, 后续研究还需对此进行相关补充及验证。

参考文献 (References)

[1] ZHAO D, LIU J, WANG M, et al. Epidemiology of cardiovascular disease in China: current features and implications [J]. Nat Rev Cardiol, 2019, 16(1): 203-12.

[2] XU S, ILYAS I, LITTLE P J, et al. Endothelial dysfunction in atherosclerotic cardiovascular diseases and beyond: from mechanism to pharmacotherapies [J]. Pharmacol Rev, 2021, 73(1): 924-67.

[3] EKHOLM M, KAHAN T. The impact of the renin-angiotensin-aldosterone system on inflammation, coagulation, and atherothrombotic complications, and to aggravated COVID-19 [J]. Front Pharmacol, 2021, 12(1): 640185.

[4] MONTAIGNE D, BUTRUILLE L, STAELS B. PPAR control of metabolism and cardiovascular functions [J]. Nat Rev Cardiol, 2021, 18(12): 809-23.

[5] ZHANG B, HAO Z, ZHOU W, et al. Formononetin protects against ox-LDL-induced endothelial dysfunction by activating PPAR-γ signaling based on network pharmacology and experimental validation [J]. Bioengineered, 2021, 12(1): 4887-98.

[6] WANG J, XU X, LI P, et al. HDAC3 protects against atherosclerosis through inhibition of inflammation via the microRNA-19b/PPARγ/NF-κB axis [J]. Atherosclerosis, 2021, 323(1): 1-12.

[7] SHEN X, ZHANG S, GUO Z, et al. The crosstalk of ABCA1 and ANXA1: a potential mechanism for protection against atherosclerosis [J]. Mol Med, 2020, 26(1): 84.

[8] XIE J, PENG L, WANG T, et al. QiShenYiQi pill inhibits atherosclerosis by promoting reverse cholesterol transport PPARγ-LXRα/β-ABCA1 pathway [J]. J Ethnopharmacol, 2023, 315(1): 116684.

[9] LIU L, TAN L, YAO J, et al. Long non-coding RNA MALAT1 regulates cholesterol accumulation in ox-LDL-induced macrophages via the microRNA-17-5p/ABCA1 axis [J]. Mol Med Rep, 2020, 21(4): 1761-70.

[10] NI J, HUANG Z, WANG D. LncRNA TP73-AS1 promotes oxidized low-density lipoprotein-induced apoptosis of endothelial cells in atherosclerosis by targeting the miR-654-3p/AKT3 axis [J]. Cell Mol Biol Lett, 2021, 26(1): 27.

[11] BOTTS S R, FISH J E, HOWE K L. Dysfunctional vascular endothelium as a driver of atherosclerosis: emerging insights into pathogenesis and treatment [J]. Front Pharmacol, 2021, 12(1): 787541.

[12] PAONE S, BAXTER A A, HULETT M D, et al. Endothelial cell apoptosis and the role of endothelial cell-derived extracellular vesicles in the progression of atherosclerosis [J]. Cell Mol Life Sci, 2019, 76(1): 1093-106.

[13] WANG X, SHEN Y, SHANG M, et al. Endothelial mechanobiology in atherosclerosis [J]. Cardiovasc Res, 2023, 119(8): 1656-75.

[14] TAMARGO I A, BAEK K I, KIM Y, et al. Flow-induced reprogramming of endothelial cells in atherosclerosis [J]. Nat Rev Cardiol, 2023, 20(11): 738-53.

[15] SHARMA A R, SHARMA G, BHATTACHARYA M, et al. Circulating miRNA in atherosclerosis: a clinical biomarker and early diagnostic tool [J]. Curr Mol Med, 2022, 22(3): 250-62.

[16] WANG H, HE F, LIANG B, et al. p53-dependent lincRNA-p21 protects against proliferation and anti-apoptosis of vascular smooth muscle cells in atherosclerosis by upregulating SIRT7 via microRNA-17-5p [J]. J Cardiovasc Transl Res, 2021, 14(3): 426-40.

[17] XU F, SHEN L, CHEN H, et al. circDENND1B participates in the antiatherosclerotic effect of IL-1β monoclonal antibody in mouse by promoting cholesterol efflux via miR-17-5p/Abca1 axis [J]. Front Cell Dev Biol, 2021, 9(1): 652032.

[18] HUANG H, PENG B, CHEN Q, et al. Long non-coding RNA nuclear-enriched abundant transcript 1 (NEAT1) facilitates foam cell formation and atherosclerosis progression through the miR-17-5p/itchy E3 ubiquitin protein ligase (ITCH)/liver kinase B1 (LKB1) axis [J]. Circ J, 2024, 88(10): 1697-708.

[19] HERNANDEZ-QUILES M, BROEKEMA M F, KALKHOVEN E. PPARgamma in metabolism, immunity, and cancer: unified and diverse mechanisms of action [J]. Front Endocrinol, 2021, 12(1): 624112.

[20] QIU X, FENG Y. Echinacoside activates Nrf2/PPARγ signaling pathway to modulate mitochondrial fusion-fission balance to ameliorate ox-LDL-induced dysfunction of coronary artery endothelial cells [J]. Naunyn Schmiedebergs Arch Pharmacol, 2024, 397(12): 9767-76.

[21] ZHANG Y, LIU K, WANG D. Notoginsenoside Fc alleviates oxidized low-density lipoprotein-induced endothelial cell dysfunction and upregulates PPAR-γ *in vitro* [J]. Histol Histopathol, 2024, 39(7): 959-67.

[22] XIE Q, PENG J, GUO Y, et al. MicroRNA-33-5p inhibits cholesterol efflux in vascular endothelial cells by regulating citrate synthase and ATP-binding cassette transporter A1 [J]. BMC Cardiovasc Disord, 2021, 21(1): 433.